Journal of Molecular Graphics and Modelling 97 (2020) 107542

Contents lists available at ScienceDirect

Journal of Molecular Graphics and Modelling

journal homepage: www.elsevier.com/locate/JMGM

Peri-, Chemo-, Regio-, Stereo- and Enantio-Selectivities of 1,3-dipolar cycloaddition reaction of C,N-Disubstituted nitrones with disubstituted 4-methylene-1,3-oxazol-5(4*H*)- one: A quantum mechanical study

George Baffour Pipim, Ernest Opoku, Richard Tia*, Evans Adei

Theoretical and Computational Chemistry Laboratory, Department of Chemistry, Kwame Nkrumah University of Science and Technology, Kumasi, Ghana

ARTICLE INFO

Article history:
Received 26 December 2019
Received in revised form
15 January 2020
Accepted 16 January 2020
Available online 21 January 2020

Keywords:
Density functional theory
1,3-Dipole
Dipolarophile
4-Methylene-1,3-oxazol-5(4*H*)-One
Spirocycloadduct

ABSTRACT

The peri-, chemo-, regio-, stereo- and enantio-selectivities of 1,3-dipolar cycloaddition reaction of C,N-disubstituted nitrones with disubstituted 4-methylene-1,3-oxazol-5(4*H*)-one have been studied using density functional theory (DFT) at the M06–2X/6-311G (d,p) level of theory. The 1,3-dipole preferentially adds chemo-selectively across the olefinic bond in a (3 + 2) fashion forming the corresponding spirocycloadduct. The titled reaction occurs with poor enantio- and stereo-selectivities, but a high degree of regio-selectivity is observed for the addition of the 1,3-dipole across the dipolarophile. Electron-withdrawing groups on the dipolarophile significantly reduce the activation barriers while electron-donating groups on the dipolarophile increase the activation barriers. Analysis of the HOMO and LUMO energies of the two reacting species indicates that the 1,3-dipole reacts as a nucleophile while the dipolarophile reacts as the electrophile. Investigation of the electrophilic Parr function (P_K^+) at the various reaction centers in the dipolarophile indicates that the 1,3-dipole selectively adds across the atomic species with the largest electrophilic Mulliken and NBO atomic spin densities which is in accordance with the energetic trends observed.

1. Introduction

Division of cycloaddition reactions is usually based on the number of new sigma bonds formed or the number of atoms linked in the ring formed [1,2]. In the most prevalent case, two reactants combine to form the cyclic compound, forming two new sigma-bonds at the expense of two pi-bonds [1,3]. Conventionally, the 1,3-dipolar cycloaddition is a reaction which involves the addition of two compounds, a dipolarophile and a 1,3-dipole to form a five-membered heterocyclic compound [1,4–6]. The 1,3-dipolar cycloaddition (1,3-DC) has become an important reaction for the construction of heterocyclic compounds of great utility in chemistry, notably, synthetic organic chemistry, material science, and chemical biology [3,7,8].

Analogous to the established Diels-Alder cycloaddition reactions, 1,3-dipolar cycloaddition reactions rely on the nucleophilic and electrophilic nature of the starting species, and the addition process is significantly impacted by the substituents present on both the 1,3-dipole and dipolarophile [9–11]. Substituents with varying electronic and stearic factors exhibit various degree of changes to energetic trends in 1,3-dipolar cycloaddition reactions [12].

The 1,3-dipole may be described as an organic molecule that possess free electrons with charge distribution across three atomic centers [1,4,13,14]. The central atom in the 1,3-dipole is usually an oxygen or a nitrogen [1]. 1,3-dipoles that have higher-row elements like sulphur and phosphorus exist but are seldomly utilized. Depending on the molecular structure, a 1,3-dipole may be classified as an allyl-type or a propargyl/allenyl type zwitterionic organic molecule [1,3].

The allyl type 1,3-dipole is described as such due to its isoelectronic character with allyl anion [3,15]. This class of 1,3-dipole has a bent geometry and possesses four electrons in the Pz orbital [13]. The central atom in allyl type 1,3-dipole can vary between group 15

* Corresponding author.
E-mail addresses: baffourgeorge88@gmail.com (G.B. Pipim), ernopoku@gmail.com (E. Opoku), richardtia.cos@knust.edu.gh, richtiagh@yahoo.com (R. Tia), eadei@yahoo.com (E. Adei).

https://doi.org/10.1016/j.jmgm.2020.107542
1093-3263/

and 16 elements. Unlike the allyl type 1,3-dipole, the propargyl/allenyl type 1,3-dipole possess a linear geometry. The central atom in propargyl/allenyl type 1,3-dipole is restricted to group 15 elements such as nitrogen [13]. Nitrones are synthetically efficient 1,3-dipoles that are basically organic molecules consisting essentially of N-oxide of an amine. Nitrones can exist as either a cyclic or acyclic molecule [1,16]. The versatility of nitrones arises from their structural diversity, their inherent selectivities in organic synthesis and utility of the resulting products primarily from 1,3-dipolar cycloaddition reactions [13,15].

Oxazolone and its derivatives are structurally distinctive collection of organic compounds that form a fragment of a large family of oxazole-based compounds [17]. Five structural isomers of oxazolone can be categorized depending on the position of the carbonyl group and the internal double bond [17,18]. Oxazolone are synthetically versatile organic molecules that are able to react with variety of nucleophiles due to their multiple electrophilic reaction centers [18]. Oxazolones provide an essential starting point for the synthesis of several important heterocyclic compounds especially of α-amino acids and peptides [19].

The synthetic application of oxazolone derivatives is far-reaching. Argyopoulos and Argyropoulou [20] reported that, the 1,3-dipolar cycloaddition reaction of nitrile oxide with 2-phenyl-4-arylidene-5(4*H*)-oxazolone chemo-selectively occurs along the olefinic bond in the oxazolone producing only one regio-isomer. Stable nitrile oxide adds across the olefinic bond of the 2-phenyl-4-arylidene-5(4*H*)-oxazolone stereospecifically and regio-selectively to yield the corresponding spirocycloadducts. Some theoretical studies on similar metal-catalysed [21–25] and metal-free [26–28] (3 + 2) cycloaddition reactions have also been reported.

In 2017, Mekheimer et al. [29] studied the 1,3-dipolar cycloaddition of 2-phenyl-4-arylidene-5(4*H*)-oxazolone (**A2**) with C-aryl (or hetearyl)-N-phenylnitrones (**A1**) in ethanol (Scheme 1). To their surprise, the reaction failed to yield the targeted spirocycloadducts **1** and **2** and the only isolable product was **4.** Based on the isolated product, they proposed that, the reaction proceed through an initial (4 + 3) cycloaddition to yield a transient intermediate (**3**) which undergoes subsequent rearrangement to form product **4** as shown in Scheme 1.

Even though this reaction provides routes to the selective synthesis of diverse synthetically and pharmaceutically vital products, the mechanism still remains unknown. In addition, the factors controlling the peri-, chemo-, regio-, stereo- and enantio-selectivities and the impact of substituents on the reactivity and the selectivities of the reactions have not been systematically studied. Also, the effects of solvents and temperature on the mechanism and hence selectivities of the reaction remains unknown. Thus, answers to the aforementioned questions on the mechanism and selectivities of the titled reaction are crucial for rational planning and execution of organic synthesis. This work therefore aims at the exhaustive theoretical exploration of the reaction pathways for the reaction of C,N-disubstituted nitrones and disubstituted 4-methylene-1,3-oxazol-5(4*H*)-one to address all the critical concerns raised above.

2. Computational details and methodology

All DFT calculations were performed with Gaussian '09 [30] quantum chemistry software packages at the M06–2X/6-311G (d,p) level of theory. The M06–2X functional developed by Zhao and Truhlar [31] has been found to be effective at computing thermochemistry and kinetics of reactions [32–34]. In the Minnesota hybrid meta-generalized gradient approximations (meta-GGA) suite of density functionals, M06–2X is among the best performing in geometry optimizations and energy calculations [35].

The initial guess structures of the considered molecules were constructed using the Spartan's graphical model builder and minimized interactively using the sybyl force field [36]. Transition state structures were computed by first obtaining guess input structures by constraining specific internal coordinates of the molecules (bond lengths, bond angles, dihedral angles) while fully optimizing the remaining internal coordinates. This procedure gives appropriate guess transition state input geometries which are then submitted for full transition state calculations without any geometry or symmetry constraints. Using the polarizable continuum model (PCM), ethanol was employed to compute solvation effects in the reactions [37]. The full optimization calculations were carried out with the Gaussian 09 package. Full harmonic vibrational frequency calculations were carried out to ensure that all transition state structures has a Hessian matrix with only a single negative eigen value, characterized by an imaginary vibrational frequency along the respective reaction coordinates. Intrinsic reaction coordinate calculations were then performed to ensure that each transition state smoothly connects the reactants and products along the reaction coordinate [38–42]. The optimized structures were illustrated using CYLview [43].

The global electrophilicities (ω) and maximum electronic charge (ΔN_{max}) of the various disubstituted 4-methylene-1,3-oxazol-5(4*H*)-one derivatives were calculated using equations (1) and (2). The electrophilicity index measures the ability of a reactant to accept electrons [10] and it has been found to be a function of the electronic chemical potential, $\mu = (E_{HOMO} + E_{LUMO})/2$ and chemical hardness, $\eta = (E_{LUMO} - E_{HOMO})$ as defined by Pearson's acid-base concept [44]. Hence, species with large electrophilicity values are more reactive towards nucleophiles. These equations are based on the Koopmans theory [45] originally established for calculating ionization energies from closed-shell Hartree–Fock wavefunctions, but have since been adopted as acceptable approximations for computing electronic chemical potential and chemical hardness.

$$\omega = \mu^2/2\eta \quad (1)$$

$$\Delta N_{max} = -\mu/\eta \quad (2)$$

The maximum electronic charge transfer (ΔN_{max}) measures the maximum electronic charge that the electrophile may accept. Thus, species with large ΔN_{max} index would be best electrophile given a series of compounds.

The global electrophilic (P_K^+) and nucleophilic (P_K^-) Parr functions were obtained through the analysis of the Mulliken and Natural Bond Orbital (NBO) atomic spin densities (ASD) of the radical anion and the radical cation by single-point energy calculations over the optimized neutral geometries using the unrestricted UM06–2X formalism for the radical species [46].

3. Results and discussion

In line with the chemo-selectivity arising from the multiple electrophilic reaction centers in 4-methylene-1,3-oxazol-5(4*H*)-one (**A2**), the 1,3-dipolar cycloaddition of C,N-disubstituted nitrone (**A1**) with disubstituted 4-methylene-1,3-oxazol-5(4*H*)-one can proceed via three dissimilar reaction pathways - either a (3 + 2) cycloaddition along in Path A and B as shown in Schemes 2 and 3 respectively or a (4 + 3) cycloaddition along Path C as shown in Scheme 3. As a result of the asymmetrical nature of the reacting species, the addition of the 1,3-dipole along the electrophilic reaction centers of the dipolarophile leads to the formation of different regio-isomers.

The (3 + 2) cycloaddition labelled in Path A arises from the

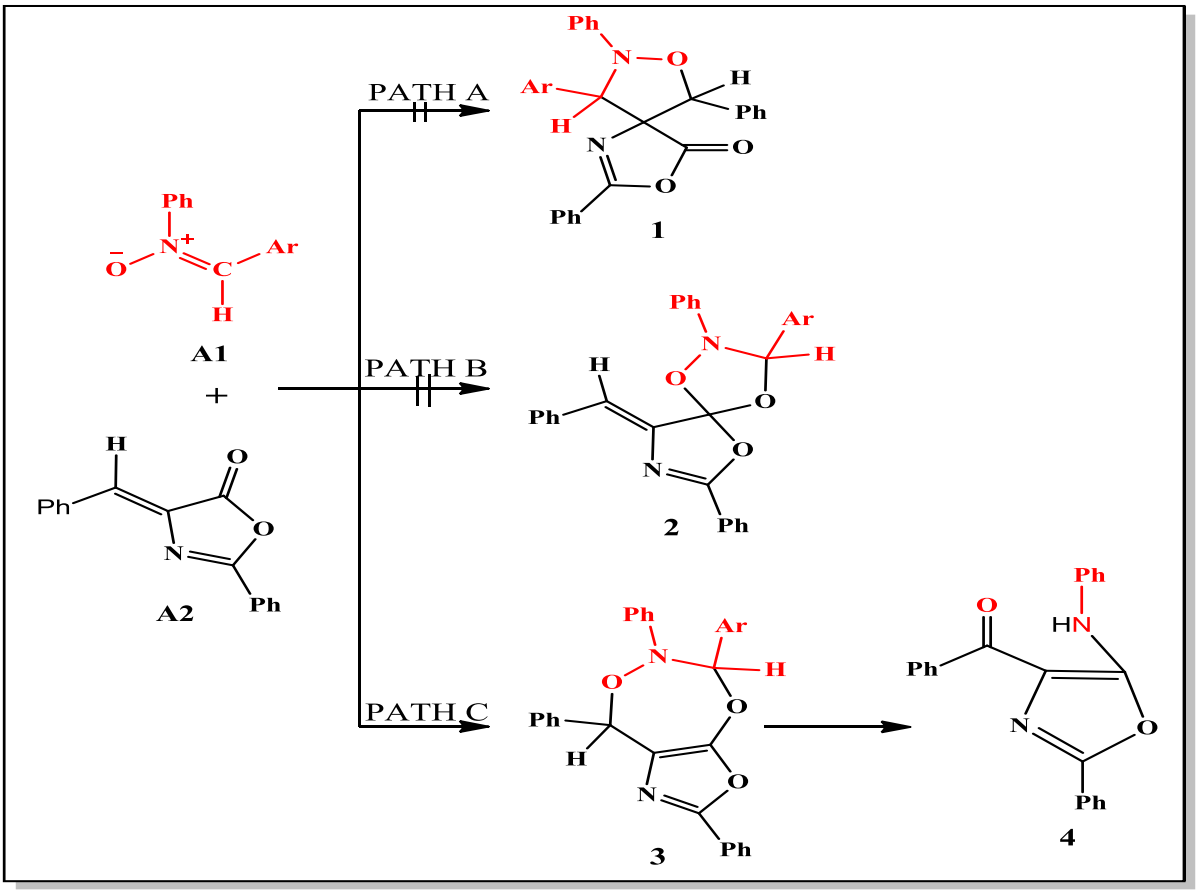

Scheme 1. 1,3-dipolar cycloaddition reaction of 2-phenyl-4-arylidene-5(4*H*)-oxazolone (**A2**) with C-aryl (or hetearyl)-N-phenylnitrones (**A1**).

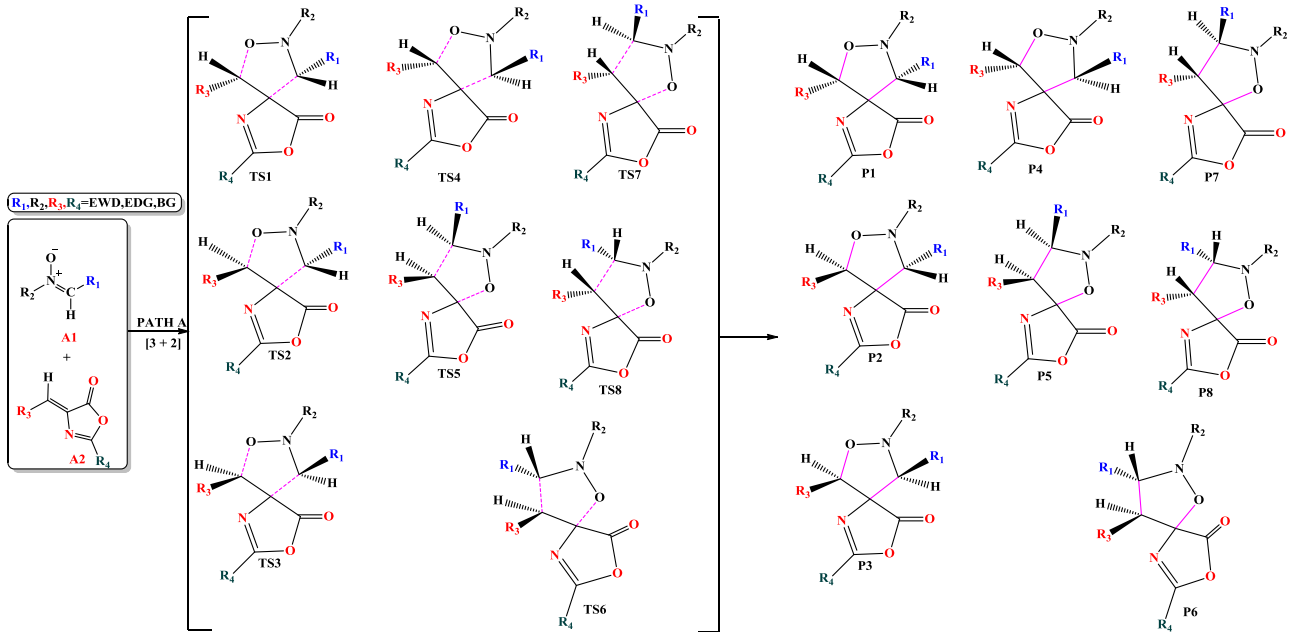

Scheme 2. Proposed scheme of study for Path A for the reaction between C,N-disubstituted nitrone with disubstituted 4 −methylene-1,3 oxazol-5(4*H*)-one.

preferential addition of the C,N disubstituted nitrone across the olefinic functionality of 4-methylene-1,3-oxazol-5(4*H*)-one. The reaction may proceed through Path A to form the spirocycloadducts (**P1**−**P8**) through the transition states (**TS1**-**TS8**). Another distinct (3 + 2) addition can proceed through Path B upon attack of the nitrone along the carbonyl bond of the 4-methylene-1,3-oxazol-5(4*H*)-one leading to the formation of four different stereo-, enantio- and regio-chemically controlled spirocycloadducts **P9**,

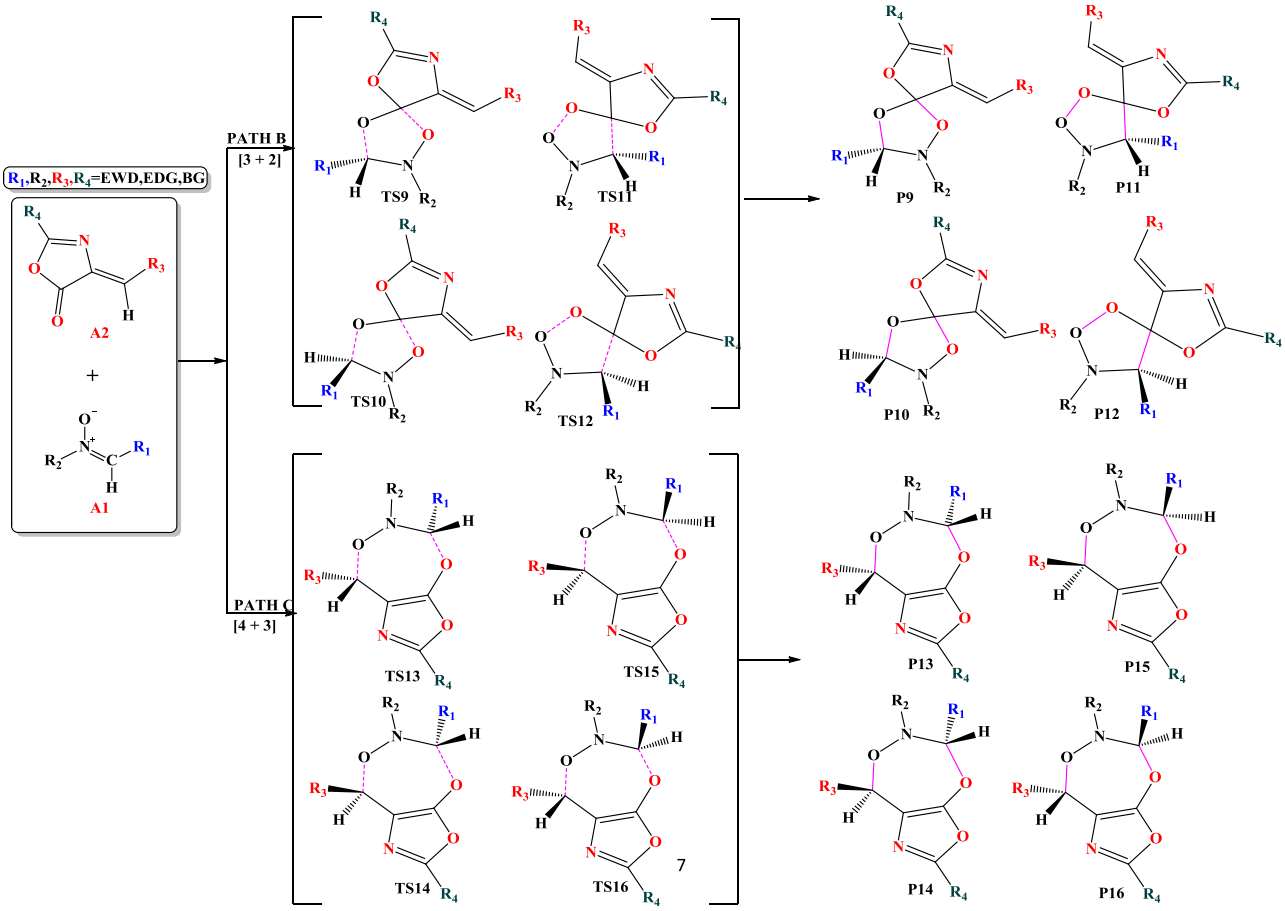

Scheme 3. Proposed scheme of study for Path B and Path C for the reaction between C,N-disubstituted nitrone with disubstituted 4 −methylene-1,3 oxazol-5(4*H*)-one.

P10, **P11** and **P12** through the transition states **TS9, TS10, TS11** and **TS12** respectively.

Selective addition of the nitrone across the methylene carbon and the carbonyl oxygen results in the (4 + 3) cycloaddition labelled in Path C. DFT calculation at M06−2X/6-311G (d,p) level of theory confirms the existence of only one possible regio-isomer. Due to the stereo- and enantio-selectivities, the reaction Path C can lead to four different products; **P13**, **P14, P15** and **P16** through transition states **TS13**, **TS14**, **TS15** and **TS16** respectively.

3.1. 1,3-DC reaction of C,N-disubstituted nitrones with disubstituted-4-methylene-1,3- oxazol-5(4H)-one

Different substituents with varying electronic and steric effects on both the 1,3-dipole and dipolarophile have been studied to investigate the possibility of affecting the mechanism of the reactions. This section examines the energetic trends and the intrinsic reactivity of the two reactants in the absence and presence of electron donating, electron withdrawing and bulky groups. The results of the analysis of dissimilar electron withdrawing groups, electron donating groups and bulky group on the reacting species is displayed in Tables 1 and 2. It ought to be mentioned that attempts to locate some transition states in selected instances proved futile. Though the possibility of those paths existing cannot be ruled out, there is a very high chance that the reactions do not proceed through these routes.

In all the reactions under consideration, the C,N-disubstituted nitrone preferentially adds across the olefinic bond of the disubstituted-4-methylene-1,3-oxazol-5(4*H*)-one. High degree of regio-selectivity is observed for the reaction via Path B and C. The formation of the spirocycloadducts **P9** and **P10** are both kinetically and thermodynamically favored over the regio-isomers **P11** and **P12**. Electron-donating groups (EDG), electron-drawing groups (EWG) and bulky group (BG) in place of hydrogens on the C,N-disubstituted nitrone and the 4-methylene-1,3-oxazol-5(4*H*)-one increase the activation barriers of the reaction with the highest barrier being 56.0 kcal/mol for amine substituted 1,3-dipole and dipolarophile while the barrier obtained for the same transition state for hydrogen substituent on 1,3-dipole and dipolarophile is 37.4 kcal/mol. Hydrogen substituents on both the 1,3-dipole and the dipolarophile leads to loss of stereo-isomerism and thus the difference in the activation barriers is as a result of regio-chemistry. Steric effect offered by phenyls on the energetics trend is minimal.

The obvious favorable pathway in terms of regio-selectivity is the Path A (Scheme 2) which leads to the formation of **P1** to **P4** through the transition states **TS1** to **TS4** respectively, which is consistent with the mechanism proposed by Argyopoulos and Argyropoulou [20]. Although in most cases, the activation barriers for the formation of **P1** to **P4** are lower relative to the activation barriers for the formation of **P5** to **P8**, the addition along the olefinic bond results in low regio-selectivity and products distribution may range from **P1** to **P8.**

In addition to the gas phase calculations, DFT calculations incorporating solvent effects (ethanol) have also been computed for the reaction of C,N-dicyano nitrone with dicyano substituted-4-methylene-1,3-oxazol-5(4*H*)-one with details displayed in Figs. 1 and 2. Similar energetic trend is observed for ethanol solvation but the magnitude of the activation barriers are appreciably higher

Table 1
Activation energies (kcal/mol) of transition states for reaction between C,N-disubstituted nitrone with disubstituted 4 −methylene-1,3 oxazol-5(4*H*)-one.

Substituents(S) ($R_1 = R_2 = R_3 = R_4 = S$)	TS1	TS2	TS3	TS4	TS5	TS6	TS7	TS8	TS9	TS10	TS11	TS12	TS13	TS14	TS15	TS16
Hydrogen	1.1	1.1	1.1	1.1	1.0	1.0	1.0	1.0	10.0	10.0	37.4	37.4	13.5	13.5	13.5	13.5
EDG																
Methyl	2.5	5.4	2.2	1.4	10.8	10.4	9.0	10.5	11.8	12.5	41.3	39.1	11.3	14.8	11.3	14.8
Ethyl	2.6	4.8	4.0	4.3	9.5	8.5	8.1	9.9	13.1	11.7	___	38.8	14.1	10.5	11.7	13.2
Amine	10.1	7.7	8.8	0.3	24.4	23.5	18.0	16.2	9.1	19.3	51.3	56.0	23.2	16.6	14.0	16.2
Hydroxyl	−0.64	0.96	28.9	22.0	4.9	14.2	4.4	9.1	17.5	12.6	43.9	47.6	14.9	19.6	24.9	9.2
Methoxy	6.6	4.7	12.6	8.8	15.5	9.2	12.5	8.5	12.6	11.8	43.4	44.2	14.1	19.0	19.0	12.2
EWD																
Cyano	7.9	7.7	4.5	3.9	5.6	6.5	5.4	4.5	8.8	10.3	38.1	40.9	21.5	23.2	24.0	22.9
Bromo	12.3	10.3	14.4	16.2	12.4	12.1	12.3	10.7	15.8	18.1	42.1	44.6	25.0	27.2	28.7	26.4
Nitro	12.5	9.1	4.9	6.3	7.0	1.7	0.7	14.5	17.0	13.9	42.5	37.7	23.2	28.5	27.3	20.9
Carbonyl	1.6	2.7	−0.75	10.0	8.1	6.0	3.5	7.8	15.7	12.6	45.0	38.6	8.3	15.7	13.7	17.0
Carboxylic acid	7.7	6.3	3.8	2.5	3.3	3.0	5.0	9.8	16.7	15.4	42.9	40.9	16.9	21.4	19.0	15.3
BG																
Phenyl	5.0	3.6	2.5	4.3	10.6	8.3	___	___	12.9	11.7	42.8	45.5	12.2	14.4	___	___

Table 2
Reaction energies (kcal/mol) of products for reaction between C,N-disubstituted nitrone with disubstituted 4 −methylene-1,3 oxazol-5(4*H*)-one.

Substituents(S) ($R_1 = R_2 = R_3 = R_4 = S$)	P1	P2	P3	P4	P5	P6	P7	P8	P9	P10	P11	P12	P13	P14	P15	P16
Hydrogen	−30.1	−30.1	−30.1	−30.1	−34.3	−34.3	−34.3	−34.3	−15.8	−15.8	33.6	33.6	−18.9	−18.9	−18.9	−18.9
EDG																
Methyl	−24.9	−26.3	−23.6	−26.8	−22.6	−25.2	−21.7	−23.5	−10.4	−10.9	42.0	41.6	−10.4	−10.6	−10.5	−10.6
Ethyl	−20.6	−23.7	−21.8	−22.0	−20.6	−25.3	−18.5	−20.5	−6.8	−10.9	42.4	42.9	−6.9	−9.4	−10.4	−9.4
Amine	−17.7	−19.1	−16.8	−15.2	−13.6	−9.9	−12.8	−11.7	−1.0	1.8	50.5	49.4	3.5	5.5	4.3	2.7
Hydroxyl	−28.8	−22.8	−31.0	−30.4	−26.2	−21.5	−22.7	−30.5	−8.8	−14.6	42.2	43.8	−9.2	−6.6	−8.6	−10.5
Methoxy	−34.2	−34.9	−27.5	−29.7	−19.9	−29.5	−22.6	−30.8	−14.8	−17.6	45.4	40.1	−12.7	−13.3	−10.1	−12.3
EWG																
Cyano	−29.6	−30.5	−31.1	−29.9	−33.8	−34.6	−32.9	−33.5	−19.3	−20.5	30.0	30.8	−18.8	−17.1	−18.6	−21.2
Bromo	−26.0	−27.5	−22.1	−25.7	−24.4	−27.7	−24.2	−28.4	−10.0	−14.5	40.3	39.8	−11.2	−9.1	−10.3	−14.4
Nitro	−42.9	−43.8	−37.8	−46.2	−40.2	−47.3	−45.9	−42.4	−17.6	−22.3	36.5	20.8	−26.1	−24.8	−29.1	−34.4
Carbonyl	−35.1	−35.8	−31.2	−29.8	−38.0	−31.6	−29.3	−32.2	−11.9	14.4	31.0	32.8	−23.7	−22.4	−24.7	−25.6
Carboxylic acid	−36.0	−34.5	−35.0	−38.1	−37.0	−41.4	−36.9	−36.1	−13.3	−15.4	37.7	33.8	−19.7	−19.3	−25.2	−26.8
BG																
Phenyl	−24.3	−22.4	−24.2	−22.5	−13.9	−23.6	−21.4	−20.5	−8.5	−10.9	40.6	40.5	−6.8	−6.0	−6.0	−5.9

for Path A and Path B whereas the activation barriers for Path C are slightly lower than the activation barriers obtained for the gas phase calculations. Activation barriers for the different reaction pathways at various temperatures for reaction of C,N-dimethyl nitrone with dimethyl-substituted-4-methylene-1,3-oxazol-5(4*H*)-one have been computed and the results displayed in Table S1. The results of the calculation indicate that temperature has no effect on the magnitude of the activation barriers and hence no effect on the energetic trend.

Highly asynchronous concerted mechanism of addition is observed for the addition of the C,N-disubstituted nitrone across disubstituted-4-methylene-1,3-oxazol-5(4*H*)-one. Principally in the (4 + 3) cycloaddition in Path C shown in Scheme 3, the bond formation between the methylene carbon of the dipolarophile and the nitrone oxygen forms with a shorter bond length in the transition state which can be attributed to the higher electron density on the two atomic species while the bond being formed between the carbonyl oxygen of the dipolarophile and the nitrone carbon proceeds with a longer bond length in the transition state. Fig. 3 is a graphical representation of optimized structures of transition states (**TS1** to **TS8**) for the reaction of C,N-dimethyl nitrone with dimethyl substituted-4-methylene-1,3-oxazol-5(4*H*)-one. The labelled bond distances confirm an asynchronous addition of the 1,3-dipole across the olefinic bond of the dipolarophile.

3.2. 1,3-DC reaction of C,N-dimethyl nitrones with disubstituted-4-methylene-1,3-oxazol- 5(4H)-one

In this section, C,N-dimethyl nitrone is used as a surrogate for C,N-diphenyl nitrone to investigate the variation in energetic trends, selectivities and reactivity that may rise from substitution of the electronically and sterically different substituents on the 4-methylene-1,3-oxazol-5(4*H*)-one. The results of the computations are displayed in Tables 3 and 4. Fig. 4 is a graphical representation of the optimized transition state structures for **TS1** to **TS8** shown in Path A in Scheme 2 for amine disubstituted 4-methylene-1,3-oxazol-5(4*H*)-one which reinforces the asynchronous addition mechanism observed for the addition of the 1,3-dipole across the dipolarophile (see Fig. 5).

Evident from the results displayed in Table 3, the addition of the C,N-dimethyl nitrone across the disubstituted-4-methylene-1,3-oxazol-5(4*H*)-one peri-selectively forms the five-membered ring over the seven-membered ring. The resulting five-membered heterocyclic compound arises from the chemo-selective (3 + 2) cycloaddition of the C,N-dimethyl nitrone across the olefinic bond of the disubstituted-4-methylene-1,3-oxazol-5(4*H*)-one labelled in Path A in Scheme 2 which is consistent with the experimental observation reported by Argyopoulos and Argyropoulou [20] but contrary to the mechanism proposed by Mekheimer et al. [29]. The (4 + 3) cycloaddition proposed by Mekheimer et al. proceeds with higher activation barrier compared to the (3 + 2) cycloaddition

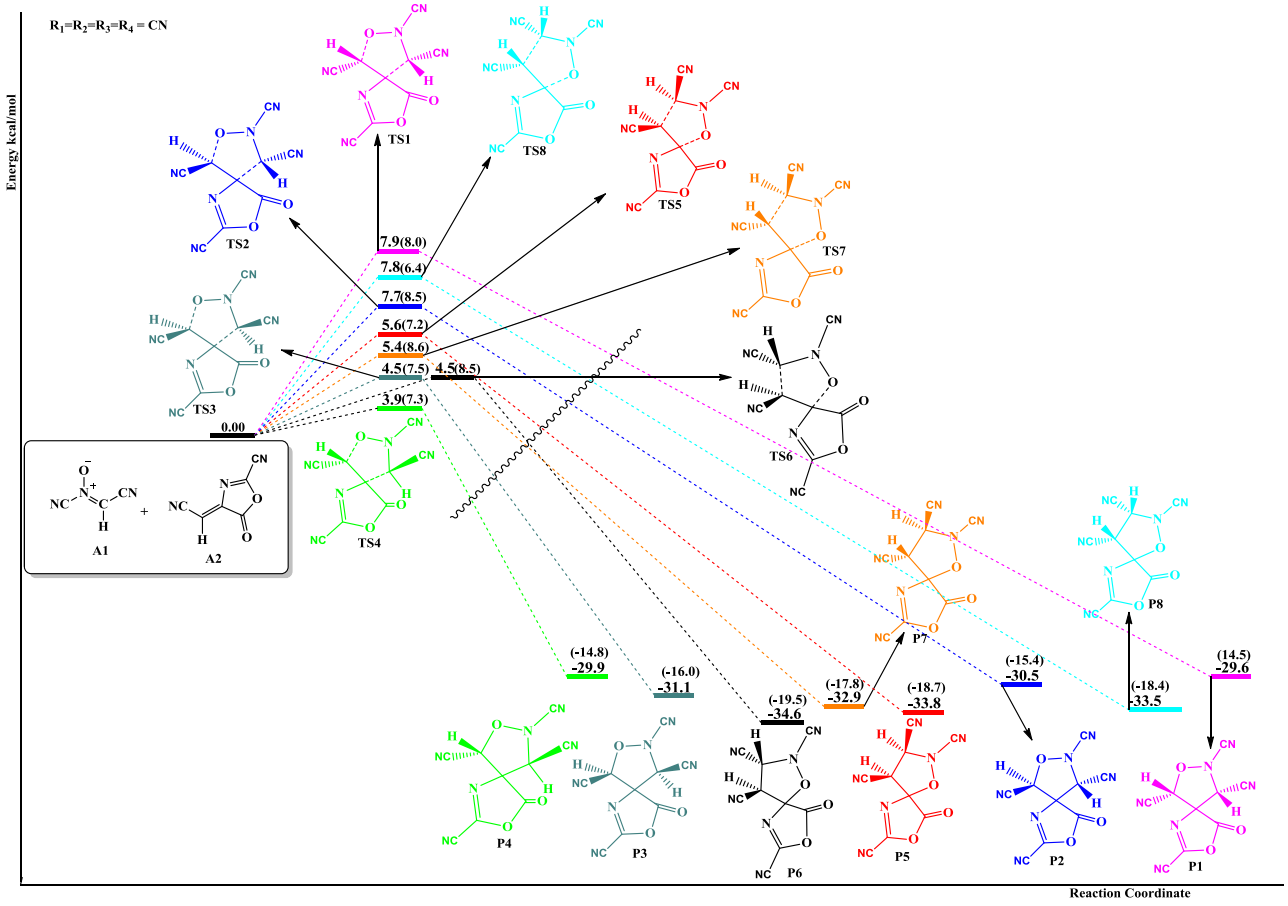

Fig. 1. Free energy profile of Path A for the reaction C,N-dicyano nitrones and dicyano subsituted-4-methylene-1,3-oxazol-5(4*H*)-on in gas phase at the at M06−2X/6-311G (d,p), level of theory. Results for computations in ethanol at 298.15 K are in parenthesis.

occurring along the olefinic bond hence the reaction will preferentially go through Path A. The (3 + 2) cycloaddition occurring along the olefinic bond regio-selectively favors the formation of **P1** to **P4** through transition states **TS1** to **TS4** respectively which can be attributed to the low steric effect experienced due to the relatively distant position of the substituents on the 1,3-dipole from the substituents on the dipolarophile. Addition of C,N-dimethyl nitrone across the carbonyl proceeds with a great regio-selectivity.

Electron-donating substituents (EDG) on the dipolarophile significantly increase the activation barriers which can be attributed to the fact that EDG increase the electron density on the dipolarophile making the dipolarophile react as a poor electrophile, while lower activation barriers result from substitution of electron-withdrawing groups on the dipolarophile owing to the fact that they withdraw electron density from the dipolarophile resulting in electron deficient dipolarophile hence making the disubstituted-4-methylene-1,3-oxazol-5(4*H*)-one react as a better electrophile. The addition of the 1,3-dipole across the dipolarophile occurs in an asynchronous fashion where the formation of one bond is more advanced than the other.

Substitution of amine groups on the 4-methylene-1,3-oxazol-5(4*H*)-one significantly increases the activation barriers compared to other substituents with the highest activation barrier of 51.0 kcal/mol. This effect is due to the ability of the amine group to donate electron density to the dipolarophile making it react as a poor electrophile and immensely increasing the activation barriers. Significant reduction in activation barriers is observed for chloro and bromo substituents on the 4-methylene-1,3-oxazol-5(4*H*)-one compared to other substituent due to its relatively stronger ability to withdraw electron density from the dipolarophile and making the dipolarophile reactive towards the 1,3-dipole and thus reducing the activation barriers.

3.3. Normal versus inverse electron demand 1,3-dipolar cycloaddition reaction

As reported in the literature [7], a 1,3-dipole may react as nucleophile where the HOMO of the 1,3-dipole couples up with the LUMO of the dipolarophile as evident in normal electron demand cycloaddition or the dipole may react as an electrophile where its LUMO couples up the HOMO of the dipolarophile in the case of inverse electron demand cycloaddition. The pairing up of the orbitals depends on the relative HOMO-LUMO energy gaps. Consequently, the rate of the reaction may be affected positively or negatively by the substituent on the reacting species which chiefly arises from alteration in the HOMO-LUMO gap. Analysis of HOMO and LUMO energies of the 1,3-dipole and dipolarophile is represented in Fig. 5. The computed LUMO energy for the 1,3-dipole (C,N-diphenyl nitrone) is −0.99eV and the HOMO is −7.05eV while that of the dipolarophile (diphenyl substituted 4-methylene-1,3-oxazol-5(4*H*)-one) is −1.87eV and −7.45eV for the LUMO and HOMO respectively. The calculated energy gap from the HOMO of the 1,3-dipole to the LUMO of the dipolarophile is 5.18eV and the energy gap from the HOMO of the dipolarophile to the LUMO of the 1,3-dipole is 6.46eV indicating that comparatively lower amount of energy is required to promote an electron from the HOMO of the

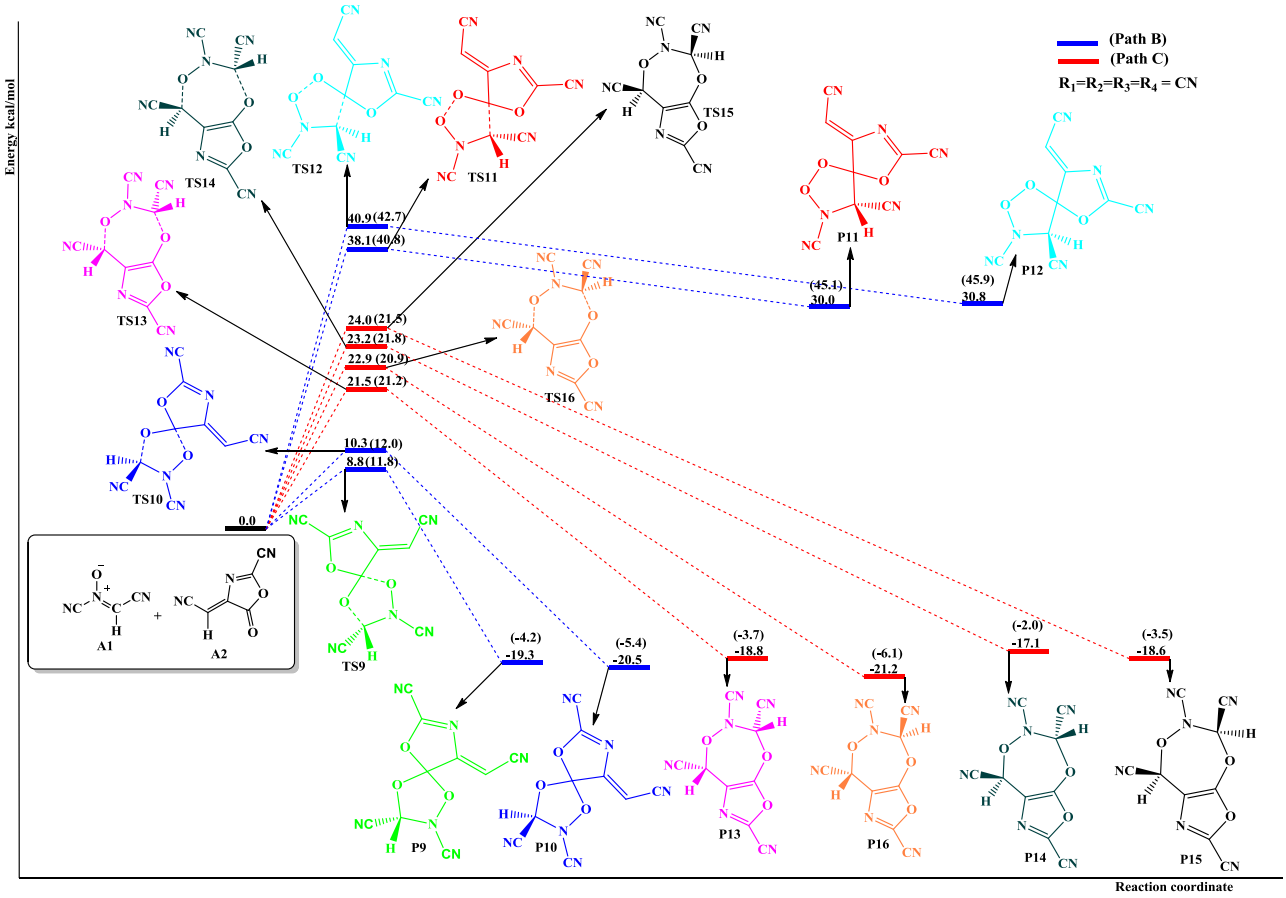

Fig. 2. Free energy profile of Path B and Path C for the reaction C,N-dicyano nitrones and dicyano substituted -4-methylene-1,3-oxazol-5(4*H*)-on in gas phase at the at M06−2X/6-311G (d,p) level of theory. Results for computations in ethanol at 298.15 K are in parenthesis.

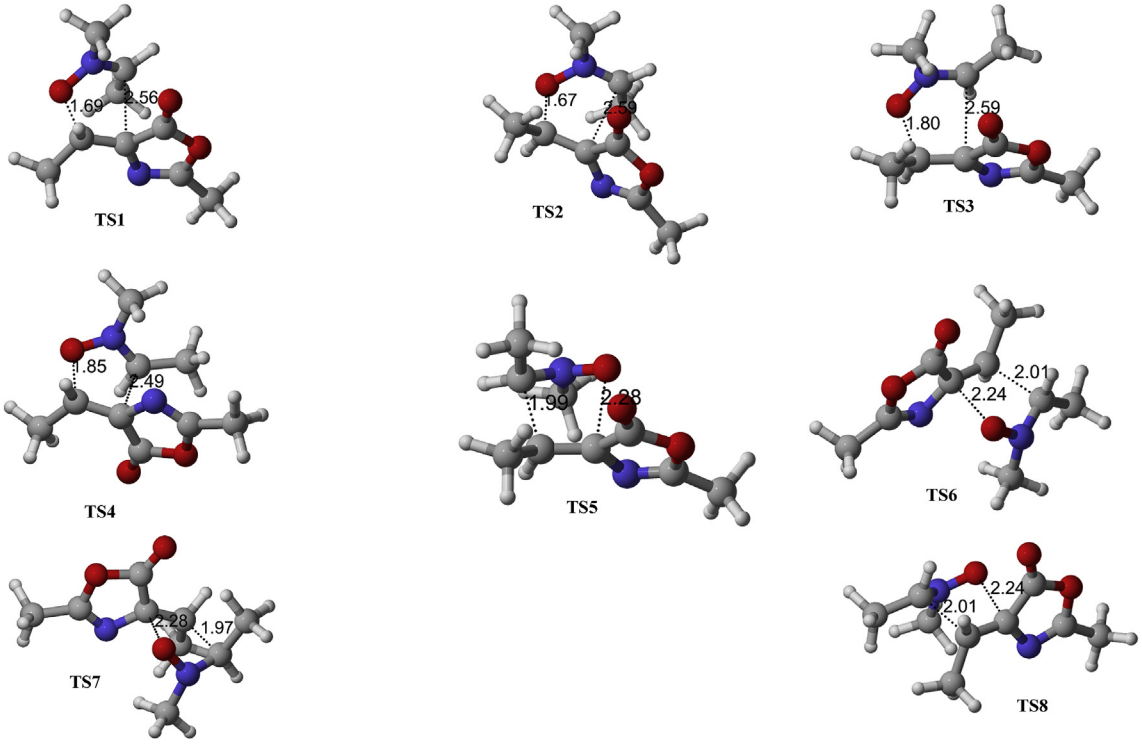

Fig. 3. Graphical representation of optimized structures for **TS1** to **TS8** for dimethyl substituted 4-methylene-1,3-oxazol-5(4*H*)-one with C,N-dimethyl nitrone.

Table 3
Activation energies (kcal/mol) of transition states for reaction between C,N-dimethyl nitrone with disubstituted 4 −methylene-1,3 oxazol-5(4*H*)-one.

Substituents(S) Table 3: Activation energies (kcal/mol) of transition states for reaction between C,N-dimethyl nitrone with disubstituted 4 −methylene-1,3 oxazol-5(4*H*)-one ($R_3 = R_4 = S$)	TS1	TS2	TS3	TS4	TS5	TS6	TS7	TS8	TS9	TS10	TS11	TS12	TS13	TS14	TS15	TS16
Hydrogen	1.3	1.3	0.22	0.22	2.5	3.7	2.5	3.7	9.5	10.0	40.3	42.0	4.9	4.9	7.7	7.7
EDG																
Amine	9.2	7.3	10.0	12.8	15.9	14.7	15.2	14.4	17.4	17.9	49.1	51.0	23.9	22.7	22.0	24.5
Hydroxyl	5.3	2.4	4.3	0.4	6.1	5.7	4.2	4.1	13.4	13.8	45.4	47.3	7.3	16.4	15.8	8.0
Methoxy	1.7	2.3	4.6	7.2	10.3	12.1	8.1	8.1	14.4	15.2	46.2	___	___	16.2	17.4	10.8
EWD																
Bromo	0.4	0.7	1.2	0.5	5.4	4.4	4.6	5.3	7.1	6.2	39.1	40.3	2.9	9.5	___	2.3
Chloro	1.8	0.4	0.5	0.4	5.5	4.4	4.2	9.1	7.1	7.7	39.3	40.3	3.0	___	8.7	2.3
BG																
Phenyl	4.1	3.3	6.4	6.8	8.0	7.2	11.1	11.4	11.7	12.5	43.2	44.9	___	15.4	14.9	12.7

Table 4
Reaction energies (kcal/mol) of products for reaction between C,N-dimethyl nitrone with disubstituted 4 −methylene-1,3 oxazol-5(4*H*)-one.

Substituents(S) Table 4: Reaction energies (kcal/mol) of products for reaction between C,N-dimethyl nitrone with disubstituted 4 −methylene-1,3 oxazol-5(4*H*)-one ($R_3 = R_4 = S$)	P1	P2	P3	P4	P5	P6	P7	P8	P9	P10	P11	P12	P13	P14	P15	P16
Hydrogen	−26.9	−26.9	−24.4	−24.4	−27.6	−28.9	−27.6	−28.9	−12.2	−12.4	40.0	39.3	−13.4	−13.4	−13.4	−13.4
EDG																
Amine	−21.7	−18.5	−16.3	−19.7	−15.6	−17.6	−16.0	−16.9	−4.9	−5.4	47.7	46.9	0.9	3.0	2.8	0.6
Hydroxyl	−32.7	−27.0	−29.8	−31.1	−25.4		−25.4	−26.4	−8.2	−8.6	44.8	44.3	−12.4	−7.1	−7.4	−12.6
Methoxy	−29.2	−27.1	−29.8	−27.1	−18.6	−20.3	−23.3	−22.3	−7.5	−7.9	45.2	44.8	−8.2	−6.8	−5.2	−8.1
EWD																
Bromo	−28.1	−28.2	−23.9	−26.5	−25.7	−28.3	−27.3	−25.0	−12.8	−13.1	39.5	39.3	−17.5	−12.4	−12.7	−9.3
Chloro	−29.1	−29.1	−27.6	−27.5	−26.3	−28.8	−27.7	−28.1	−13.0	−13.3	39.4	39.2	−17.5	−12.7	−13.0	−17.7
BG																
Phenyl	−21.3	−22.2	−19.3	−19.5	−17.8	−22.3	−20.8	−18.6	−9.5	−10.0	42.8	42.3	−7.0	−5.6	−5.6	−7.1

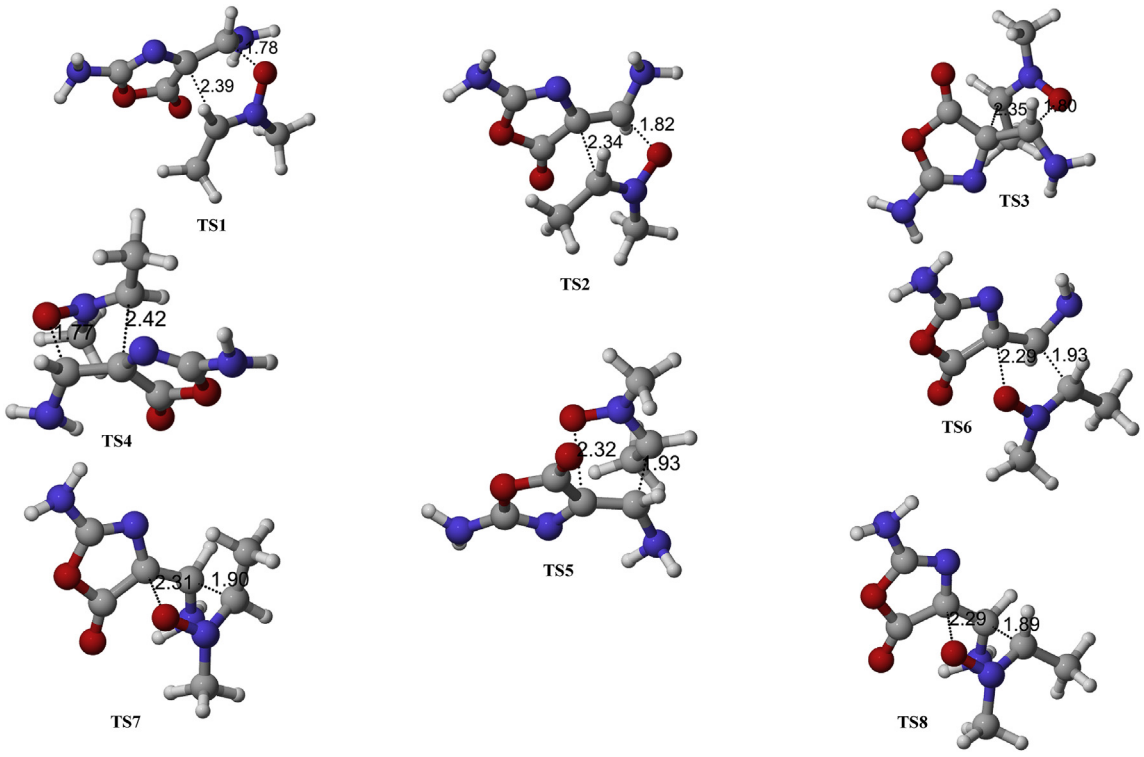

Fig. 4. Graphical representation of optimized structures for **TS1** to **TS8** for amine disubstituted 4-methylene-1,3-oxazol-5(4H)-one with C,N-dimethyl nitrone.

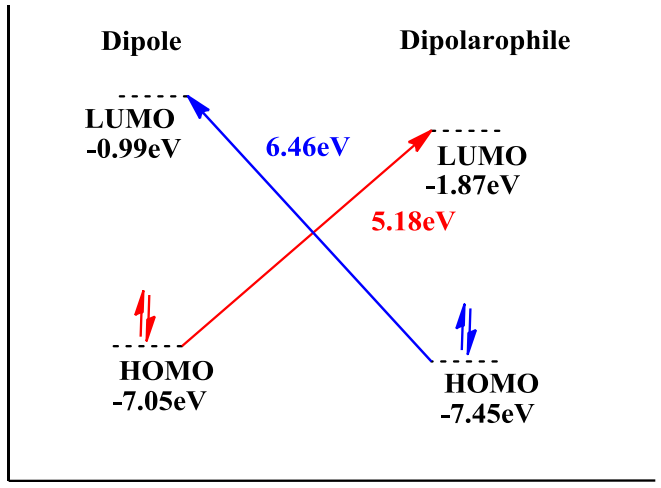

Fig. 5. Graphical depiction of the HOMO-LUMO gap of C,N-diphenyl nitrone and diphenyl substituted 4-methylene-1,3-oxazol-5(4*H*)-one.

1,3-dipole to the LUMO of the dipolarophile. The reaction thus proceeds as a normal electron demand cycloaddition with the dipolarophile reacting as an electrophile and the 1,3-dipole reacting as a nucleophile hence electron withdrawing groups on the dipolarophile and electron donating groups on the 1,3-dipole will significantly lower the activation barriers of the reaction.

3.4. Analysis of the reaction with global reactivity indices

The intrinsic reactivity of a species is affected by the nature of the substituents on it. Variation in the reactivity of species immensely affects the rate at which reactions proceed. The global reactivity index (ω) and maximum charge transfer (ΔN_{max}) are effective parameters for rationalizing the relative nucleophilicity and electrophilicity of reactants that arise from variation of substituents on the reactants. The ability of a species to accept electrons and the maximum charge an electrophile can carry in a chemical reaction is described by the electrophilicity index and the maximum charge transfer respectively. Thus, in a series of reactants, the species with the largest electrophilicity index and maximum charge transfer values is the best electrophile while species with the smallest values is the best nucleophile. Evident from Table 5, the electrophilicities of the various derivatives of 4-methylene-1,3-oxazol-5(4*H*)-one is given in the order Br = Cl > Ph > H > OMe > OH > NH_2 with amine derivative having the smallest value of 0.8 as anticipated thus reacting as poorest electrophile among the various derivatives which is consistent with the energetic trends observed in the reaction of various derivatives of 4-methylene-1,3-oxazol-5(4*H*)-one with the C,N-dimethyl nitrone. Similar trend is observed for the ΔN_{max} calculations for the various derivatives where the substrate with the largest value is found to have the lower activation barriers.

3.5. Origin of selectivity: local reactivity indices

The local electrophilic (P_K^+) and nucleophilic (P_K^-) Parr functions are employed to rationalize the preferential addition of the 1,3-dipole across the dipolarophile. Both Mulliken and NBO atomic spin densities (ASD) are invoked to rationalize the selectivity observed in the titled reaction and these analyses give a quantitative measure of the electron density at various atomic centers. Within a dipolarophile, atomic species with largest electron densities are the ideal point of attack by the 1,3-dipole. The origin of

Table 5
Global reactivity indices for the various derivatives of 4-methylen-1,3-oxazol-5(4*H*)-one. Orbital Energies are in eV.

SUBSTRATE	HOMO	LUMO	μ	η	ω	ΔN_{max}
Hydrogen	−8.95	−1.44	−5.20	7.51	1.80	0.69
Amine	−6.66	0.09	−3.28	6.75	0.80	0.49
Hydroxyl	−7.77	−0.57	−4.20	7.20	1.21	0.58
Methoxy	−7.51	−0.48	−4.00	7.03	1.13	0.57
Bromo	−8.67	−1.94	−5.31	6.74	2.10	0.79
Chloro	−8.86	−1.92	−5.39	6.94	2.10	0.78
Phenyl	−7.45	−1.87	−4.66	5.58	1.94	0.83

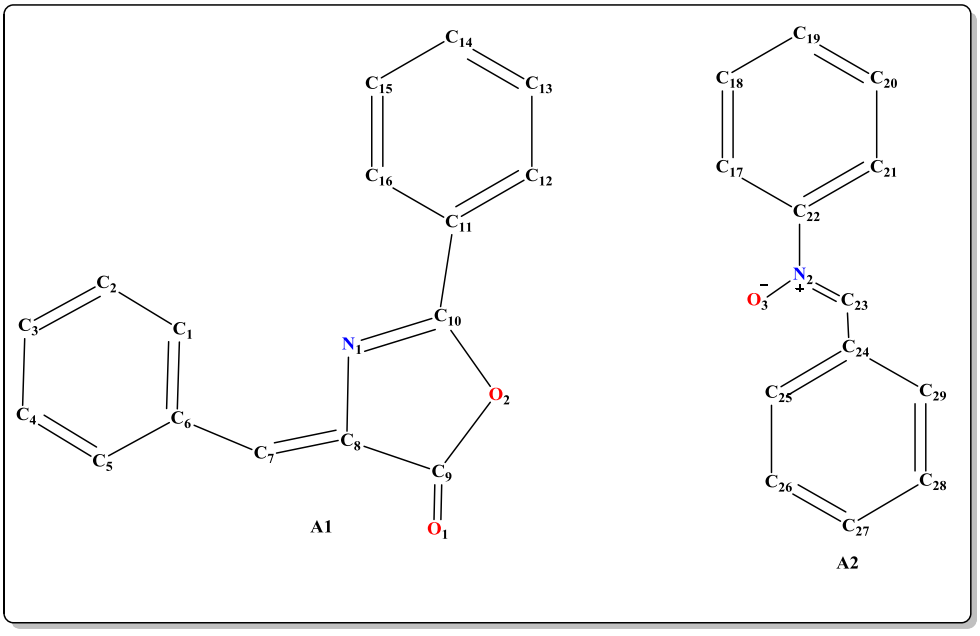

Fig. 6. Atomic labels of the C,N-diphenyl nitrone (**A2**) and diphenyl substituted 4-methylene-1,3-oxazol-5(4*H*)-one (**A1**).

Table 6
Mulliken and NBO atomic spin densities of C,N-diphenyl nitrone (1,3-dipole) and diphenyl substituted 4-methylene-1,3-oxazol-5(4*H*)-one (dipolarophile).

DIPOLAROPHILE			1,3-DIPOLE			DIPOLAROPHILE			1,3-DIPOLE		
	NBO			NBO			MULLIKEN			MULLIKEN	
	ANION	CATION		ANION	CATION		ANION	CATION		ANION	CATION
C_1	0.117	0.099	C_{17}	0.079	0.021	C_1	0.141	0.117	C_{17}	0.091	0.023
C_2	−0.044	−0.043	C_{18}	−0.030	−0.007	C_2	−0.069	−0.068	C_{18}	−0.044	−0.011
C_3	0.138	0.185	C_{19}	0.142	0.041	C_3	0.168	0.218	C_{19}	0.163	0.047
C_4	−0.039	−0.046	C_{20}	−0.044	−0.013	C_4	−0.060	−0.071	C_{20}	−0.061	−0.018
C_5	0.095	0.104	C_{21}	0.101	0.027	C_5	0.112	0.121	C_{21}	0.117	0.033
C_6	−0.038	0.039	C_{22}	0.025	0.001	C_6	−0.077	0.022	C_{22}	0.018	−0.022
C_7	0.320	0.143	C_{23}	0.192	0.150	C_7	0.377	0.155	C_{23}	0.207	0.157
C_8	0.013	0.157	C_{24}	−0.012	0.041	C_8	−0.007	0.157	C_{24}	−0.032	0.036
C_9	0.050	−0.025	C_{25}	0.105	0.087	C_9	0.053	−0.035	C_{25}	0.121	0.094
C_{10}	0.196	0.058	C_{26}	−0.044	−0.036	C_{10}	0.216	0.068	C_{26}	−0.062	−0.053
C_{11}	−0.022	0.012	C_{27}	0.157	0.178	C_{11}	−0.047	0.006	C_{27}	0.183	0.202
C_{12}	0.079	0.039	C_{28}	−0.048	−0.047	C_{12}	0.096	0.045	C_{28}	−0.066	−0.066
C_{13}	−0.031	−0.015	C_{29}	0.106	0.103	C_{13}	−0.049	−0.025	C_{29}	0.120	0.114
C_{14}	0.106	0.075	O_3	0.148	0.419	C_{14}	0.129	0.090	O_3	0.147	0.416
C_{15}	−0.031	−0.022	N_2	0.145	0.054	C_{15}	−0.049	−0.034	N_2	0.139	0.054
C_{16}	0.079	0.047				C_{16}	0.097	0.056			
O_1	0.077	0.080				O_1	0.075	0.082			
O_2	−0.016	0.001				O_2	−0.023	0.001			
N_1	−0.020	0.135				N_1	−0.032	0.128			

selectivity is investigated with C,N-diphenyl nitrone and diphenyl substituted 4-methylene-1,3-oxazol-5(4*H*)-one. The results of the analyses are displayed in Table 6. Atomic labels of the 1,3-dipole (C,N-diphenyl nitrone) and dipolarophile (and diphenyl substituted 4-methylene-1,3-oxazol-5(4*H*)-one) are displayed in Fig. 6. Analysis of the multiple reaction centers in the dipolarophile indicates that, pertaining to the electrophilic Mulliken spin densities, $C_7 = 0.143$, $C_8 = 0.157$, $C_9 = -0.0245$ and $O_1 = 0.080$ indicating that the 1,3-dipole will preferentially add across the C_7 and C_8 atoms as in the case of Path A in Scheme 2. This observation is consistent with the energetic trend observed for reaction of C,N-disubstituted nitrones with disubstituted-4-methylene-1,3-oxazol-5(4*H*)-one. Similar observation is made for NBO atomic spin density analysis.

4. Conclusion

The results of the study indicate that the 1,3-dipolar cycloaddition of C,N-disubstituted nitrone with disubstituted 4-methylene-1,3-oxazol-5(4*H*)-one peri-selectively leads to the formation of the five-membered heterocyclic ring through the $(3 + 2)$ cycloaddition rather than the seven-membered ring that proceeds through the $(4 + 3)$ cycloaddition. The 1,3-dipole chemo-selectively adds across the olefinic bond instead of the carbonyl bond. The reaction proceeds with poor stereo- and enantio-selectivities but high degree of regio-selectivity is observed for addition of the 1,3-dipole across the carbonyl group in the dipolarophile and the $(4 + 3)$ cycloaddition along the methylene carbon and the carbonyl oxygen of the dipolarophile.

Electron-donating groups on the dipolarophile significantly increase the activation barriers, unlike electron-withdrawing groups which decrease the activation barriers for the reaction of C,N-dimethyl nitrone with various derivatives of 4-methylene-1,3-oxazol-5(4*H*)-one. The species with highest electrophilicity index in a series of disubstituted 4-methylene-1,3-oxazol-5(4*H*)-one will react as the best electrophile and will have significantly low activation barriers. Ethanol solvation has no substantial effect on the observed energetic trends in the gas phase but rather there is an appreciable variation in the magnitude of the activation energy from the observed energies in the gas phase calculations and the resulting spirocycloadducts are thermodynamically less stable in ethanol than in the gas phase. Temperature has no effect on the magnitude of the activation barriers and the hence no effect on the observed energetic patterns.

Declaration of competing interest

The authors declare that there is no conflict of interests whatsoever regarding the publication of this manuscript.

Acknowledgements

The authors are very grateful to the National Council for Tertiary Education, Republic of Ghana, for a research grant under the Teaching and Learning Innovation Fund (TALIF/KNUST/3/0008/2005), and to South Africa's Centre for High Performance Computing for access to additional computing resource on the lengau cluster.

Appendix A. Supplementary data

Supplementary data to this article can be found online at https://doi.org/10.1016/j.jmgm.2020.107542.

References

[1] B.D. Prof, Rolf huisgen, chemischen industric, dusscldorf, Angew. Chern. Interntrf. Ed. 23 (1961) 1.
[2] M. Lautens, W. Klute, W. Tam, Transition metal-mediated cycloaddition reactions, Chem. Rev. 96 (1996) 49–92.
[3] T. Hashimoto, K. Maruoka, Recent advances of catalytic asymmetric 1,3-dipolar cycloadditions, Chem. Rev. 115 (2015) 5366–5412, https://doi.org/10.1021/cr5007182.
[4] G. Arhin, A.H. Adams, E. Opoku, R. Tia, E. Adei, 1, 3-Dipolar cycloaddition reactions of selected 1,3-dipoles with 7-isopropylidenenorbornadiene and follow-up thermolytic cleavage: a computational study, J. Mol. Graph. Model. 92 (2019) 267–279, https://doi.org/10.1016/j.jmgm.2019.08.004.
[5] M. Freindorf, T. Sexton, The Mechanism of the Cycloaddition Reaction of 1 , 3-dipole Molecules with Acetylene : an Investigation with the Unified Reaction Valley Approach, 2014, https://doi.org/10.1007/s00214-013-1423-z.
[6] E. Opoku, G. Arhin, G.B. Pipim, A.H. Adams, R. Tia, E. Adei, Site-, enantio- and stereo-selectivities of the 1,3-dipolar cycloaddition reactions of oxanorbornadiene with C,N-disubstituted nitrones and dimethyl nitrilimines: a DFT mechanistic study, Theor. Chem. Acc. 139 (2020) 16, https://doi.org/10.1007/s00214-019-2529-8.
[7] P. Merino, J. Revuelta, T. Tejero, U. Chiacchio, A. Rescifina, G. Romeo, A DFT study on the 1,3-dipolar cycloaddition reactions of C-(methoxycarbonyl)-N-

methyl nitrone with methyl acrylate and vinyl acetate, Tetrahedron 59 (2003) 3581–3592, https://doi.org/10.1016/S0040-4020(03)00547-7.
[8] M.J. Aurell, L.R. Domingo, P. Pérez, R. Contreras, A theoretical study on the regioselectivity of 1,3-dipolar cycloadditions using DFT-based reactivity indexes, Tetrahedron 60 (2004) 11503–11509, https://doi.org/10.1016/j.tet.2004.09.057.
[9] S. Mandal, K.K. Maiti, A. Banerji, T. Prangé, A. Neuman, N. Acharjee, Experimental and DFT studies for substituent effects on cycloadditions of C, N-disubstituted nitrones to cinnamoyl piperidine 57 (2018) 108–119.
[10] Luis R. Domingo, M. José Aurell, Patricia Pérez, Renato Contreras, Quantitative Characterization of the Local Electrophilicity of Organic Molecules, Understanding the Regioselectivity on Diels–Alder Reactions, 2002, https://doi.org/10.1021/JP020715J.
[11] D.H. Ess, K.N. Houk, Theory of 1 , 3-dipolar Cycloadditions : distortion/interaction and frontier molecular orbital models, J. Am. Chem. Soc. 130 (131) (2008) 10187–10198.
[12] M. Mensah, E.E. Amepetey, R. Tia, E. Adei, 1,3-Dipolar [3 + 2] cycloaddition reactions of N,C,C-trisubstituted nitrones with ring-acceptor methylenecyclopropanes: a computational study, SpringerPlus 5 (2016) 2072, https://doi.org/10.1186/s40064-016-3758-0.
[13] M. Kissane, A.R. Maguire, Asymmetric 1,3-dipolar cycloadditions of acrylamides, Chem. Soc. Rev. 39 (2010) 845–883, https://doi.org/10.1039/b909358n.
[14] S. Nantogma, R. Tia, E. Adei, A DFT mechanistic study of the generation of azomethine ylides from the ring-opening reactions of stabilized aziridines and follow-up 1,3-dipolar cycloaddition reactions with acetaldehyde, Comput, Theor. Chem. 1144 (2018) 38–49, https://doi.org/10.1016/J.COMPTC.2018.10.002.
[15] L.M. Stanley, M.P. Sibi, Enantioselective copper-catalyzed 1 , 3-dipolar cycloadditions, Chem. Rev. 108 (8) (2008) 2887–2902.
[16] S.I. Murahashi, Y. Imada, Synthesis and transformations of nitrones for organic synthesis, Chem. Rev. 119 (2019) 4684–4716, https://doi.org/10.1021/acs.chemrev.8b00476.
[17] A.K. Mukerjee, Azlactones: retrospect and prospect, Heterocycles 26 (1987) 1077, https://doi.org/10.3987/r-1987-04-1077.
[18] A.S.A. Youssef, F.A. El-Mariah, F.T. Abd-Elmottaleb, H.E. Hashem, Reaction of 2-Phenyl-4-arylidene-1,3-oxazolones with different nucleophiles for synthesis of some new heterocycles, J. Heterocycl. Chem. 56 (2019) 456–463, https://doi.org/10.1002/jhet.3419.
[19] S.W. King, J.M. Riordan, E.M. Holt, C.H. Stammer, Synthesis of racemic (E)-and (Z)-1-amino-2-phenylcyclopropanecarboxylic acid:(E)-and (Z)-cyclopropylphenylalanine, J. Org. Chem. 47 (17) (1982) 3270–3273.
[20] N.G. Argyropoulos, C.A. Evdoxia, 1, 3-Dipolar cycloaddition reactions of 2-phenyl-4-arylidene-5 (4H)-oxazolones with nitrile oxides, J. Het. Chem. 2 (5) (1984) 1397–1400.
[21] A.S. Novikov, M.L. Kuznetsov, Theoretical study of Re(IV) and Ru(II) bis-isocyanide complexes and their reactivity in cycloaddition reactions with nitrones, Inorg. Chim. Acta. 380 (2012) 78–89, https://doi.org/10.1016/j.ica.2011.08.016.
[22] A.S. Novikov, M.L. Kuznetsov, A.J.L. Pombeiro, Theory of The formation and decomposition of N-heterocyclic aminooxycarbenes through metal-assisted [2+3]-Dipolar cycloaddition/retro-cycloaddition, Chem. Eur J. 19 (2013) 2874–2888, https://doi.org/10.1002/chem.201203098.
[23] A.S. Novikov, 1,3-Dipolar cycloaddition of nitrones to transition metal-bound isocyanides: DFT and HSAB principle theoretical model together with analysis of vibrational spectra, J. Organomet. Chem. 797 (2015) 8–12, https://doi.org/10.1016/J.JORGANCHEM.2015.07.024.
[24] M.A. Kinzhalov, A.S. Novikov, K.V. Luzyanin, M. Haukka, A.J.L. Pombeiro, V.Y. Kukushkin, PdII-mediated integration of isocyanides and azide ions might proceed via formal 1,3-dipolar cycloaddition between RNC ligands and uncomplexed azide, New J. Chem. 40 (2016) 521–527, https://doi.org/10.1039/c5nj02564h.
[25] M.A. Kinzhalov, A.S. Legkodukh, T.B. Anisimova, A.S. Novikov, V.V. Suslonov, K.V. Luzyanin, V.Y. Kukushkin, Tetrazol-5-ylidene gold(III) complexes from sequential [2 + 3] cycloaddition of azide to metal-bound isocyanides and N4 alkylation, Organometallics 36 (2017) 3974–3980, https://doi.org/10.1021/acs.organomet.7b00591.
[26] E.V. Sirotkina, M.M. Efremova, A.S. Novikov, V.V. Zarubaev, I.R. Orshanskaya, G.L. Starova, R.R. Kostikov, A.P. Molchanov, Regio- and diastereoselectivity of the cycloaddition of aldonitrones with benzylidenecyclopropane: an experimental and theoretical study, Tetrahedron 73 (2017) 3025–3030, https://doi.org/10.1016/J.TET.2017.04.014.
[27] V.A. Dmitriev, M.M. Efremova, A.S. Novikov, V.V. Zarubaev, A.V. Slita, A.V. Galochkina, G.L. Starova, A.V. Ivanov, A.P. Molchanov, Highly efficient and stereoselective cycloaddition of nitrones to indolyl- and pyrrolylacrylates, Tetrahedron Lett. 59 (2018) 2327–2331, https://doi.org/10.1016/j.tetlet.2018.04.066.
[28] M.M. Efremova, A.S. Novikov, R.R. Kostikov, T.L. Panikorovsky, A.V. Ivanov, A.P. Molchanov, Regio- and diastereoselectivity of the cycloaddition of nitrones with N-propadienylindole and pyrroles, Tetrahedron 74 (2018) 174–183, https://doi.org/10.1016/j.tet.2017.11.056.
[29] R.A. Mekheimer, K. Al-Zaydi, M.A.A. Ibrahim, A. Al-Shamary, K. Sadek, Regio- and stereoselective 1,3-dipolar cycloaddition reactions of C-aryl (or hetaryl)-N-phenylnitrones to monosubstituted ylidene malononitriles and 4-benzylidene-2-phenyloxazol-5(4H)-one, Zeitschrift Fur Naturforsch. - Sect. B J. Chem. Sci. 72 (2017) 317–326, https://doi.org/10.1515/znb-2016-0263.
[30] M.J. Frisch, G.W. Trucks, H.B. Schlegel, G.E. Scuseria, M.A. Robb, J.R. Cheeseman, G. Scalmani, V. Barone, B. Mennucci, G.A. Petersson, H. Nakatsuji, M. Caricato, X. Li, H.P. Hratchian, A.F. Izmaylov, J. Bloino, G. Zheng, J.L. Sonnenberg, M. Hada, M. Ehara, K. Toyota, R. Fukuda, J. Hasegawa, M. Ishida, T. Nakajima, Y. Honda, O. Kitao, H. Nakai, T. Vreven, J.A. Montgomery, J.E. Peralta, F. Ogliaro, M. Bearpark, J.J. Heyd, E. Brothers, K.N. Kudin, V.N. Staroverov, R. Kobayashi, J. Normand, K. Raghavachari, A. Rendell, J.C. Burant, S.S. Iyengar, J. Tomasi, M. Cossi, N. Rega, J.M. Millam, M. Klene, J.E. Knox, J.B. Cross, V. Bakken, C. Adamo, J. Jaramillo, R. Gomperts, R.E. Stratmann, O. Yazyev, A.J. Austin, R. Cammi, C. Pomelli, J.W. Ochterski, R.L. Martin, K. Morokuma, V.G. Zakrzewski, G.A. Voth, P. Salvador, J.J. Dannenberg, S. Dapprich, A.D. Daniels, Ö. Farkas, J.B. Foresman, J.V. Ortiz, J. Cioslowski, D.J. Fox, Gaussian 09, Revision B. 01, Gaussian Inc., Wallingford, CT, 2009 6492.
[31] Y. Zhao, D.G. Truhlar, Density functionals with broad applicability in chemistry, Acc. Chem. Res. 41 (2008) 157–167, https://doi.org/10.1021/ar700111a.
[32] S.N. Pieniazek, K.N. Houk, The origin of the halogen effect on reactivity and reversibility of diels–alder cycloadditions involving furan, Angew. Chem. Int. Ed. 45 (2006) 1442–1445, https://doi.org/10.1002/anie.200502677.
[33] R.S. Paton, J.L. Mackey, W.H. Kim, J.H. Lee, S.J. Danishefsky, K.N. Houk, Origins of stereoselectivity in the *trans* Diels–Alder paradigm, J. Am. Chem. Soc. 132 (2010) 9335–9340, https://doi.org/10.1021/ja1009162.
[34] R.S. Paton, S.E. Steinhardt, C.D. Vanderwal, K.N. Houk, Unraveling the mechanism of cascade reactions of zincke aldehydes, J. Am. Chem. Soc. 133 (2011) 3895–3905, https://doi.org/10.1021/ja107988b.
[35] S.E. Wheeler, A. Moran, S.N. Pieniazek, K.N. Houk, Accurate reaction enthalpies and sources of error in DFT thermochemistry for aldol, mannich, and α-aminoxylation reactions, J. Phys. Chem. 113 (2009) 10376–10384, https://doi.org/10.1021/jp9058565.
[36] M. Clark, R.D. Cramer, N. Van Opdenbosch, Validation of the general purpose tripos 5.2 force field, J. Comput. Chem. 10 (1989) 982–1012, https://doi.org/10.1002/jcc.540100804.
[37] J. Tomasi, B. Mennucci, R. Cammi, Quantum mechanical continuum solvation models, Chem. Rev. 105 (2005) 2999–3093, https://doi.org/10.1021/cr9904009.
[38] E. Opoku, R. Tia, E. Adei, Computational studies on [4+2]/[3+2] tandem sequential cycloaddition reactions of functionalized acetylenes with cyclopentadiene and diazoalkane for the formation of norbornene pyrazolines, J. Mol. Model. 25 (2019) 168, https://doi.org/10.1007/s00894-019-4056-x.
[39] E. Opoku, R. Tia, E. Adei, DFT mechanistic study on tandem sequential [4 + 2]/[3 + 2] addition reaction of cyclooctatetraene with functionalized acetylenes and nitrile imines, J. Phys. Org. Chem. (2019), e3992, https://doi.org/10.1002/poc.3992.
[40] E. Opoku, R. Tia, E. Adei, Quantum chemical studies on the mechanistic aspects of tandem sequential cycloaddition reactions of cyclooctatetraene with ester and nitrones, J. Mol. Graph. Model. 92 (2019) 17–31, https://doi.org/10.1016/J.JMGM.2019.06.019.
[41] E. Opoku, R. Tia, E. Adei, [3 + 2] versus [2 + 2] Addition : a density functional theory study on the mechanistic aspects of transition metal-assisted formation of 1 , 2-dinitrosoalkanes, J. Chem. 2016 (2016) 10, https://doi.org/10.1155/2016/4538696.
[42] D. Roland, J.N. Haleegoah, E. Opoku, R. Tia, E. Adei, Mechanistic studies on tandem cascade [4 + 2]/[3 + 2] cycloaddition of 1,3,4-oxadiazoles with olefins, J. Mol. Graph. Model. 93 (2019), 107452, https://doi.org/10.1016/j.jmgm.2019.107452.
[43] C.Y. Legault, C.Y. CYLview. http://www.cylview.org, 2009.
[44] R.G. Parr, L.v. Szentpály, S. Liu, Electrophilicity index, J. Am. Chem. Soc. 121 (1999) 1922–1924, https://doi.org/10.1021/ja983494x.
[45] T. Koopmans, Über die Zuordnung von Wellenfunktionen und Eigenwerten zu den Einzelnen Elektronen Eines Atoms, Physica 1 (1934) 104–113, https://doi.org/10.1016/S0031-8914(34)90011-2.
[46] L.R. Domingo, P. Pérez, J.A. Sáez, Understanding the local reactivity in polar organic reactions through electrophilic and nucleophilic Parr functions, RSC Adv. 3 (2013) 1486–1494, https://doi.org/10.1039/c2ra22886f.